Experimental Mechanics at Velocity Extremes —Very High Strain Rates

Study covers tensile and compression specimens, spherical bulging and cylindrical bulging for a wide variety of materials

by W. W. Wood

ABSTRACT—The early experimental work of Clark and Wood with regard to von Kármán's theory on the effect of material flow and fracture at high strain rates has led to many controversial issues on these effects. Interest has been greatly revived in recent years because of the increased emphasis on such high-velocity forming processes as explosive and capacitor discharge. Considerable new work has been performed by Ling-Temco-Vought, Inc., for the Air Force, the results of which are presented in this paper. Data have been accumulated on tensile and compression specimens, spherical bulging and cylindrical bulging for a wide variety of materials. This high-speed information has been generated with the use of a special projectile impact machine and special presses utilizing various combinations of explosive and capacitor-discharge energy, with strain rates to 10^4/sec. The effect of velocity on ductility is discussed for total strain distribution, uniform strain, double necking and critical impact velocity. The modes of failure for various part shapes are presented and related to the forming velocity.

W. W. Wood is Chief of Manufacturing, Research and Development, LTV Vought Aeronautics Division, Dallas, Tex.

Paper was presented at 1965 SESA Spring Meeting held in Denver, Colo., on May 5–7.

Explosive Forming

As shown in Fig. 1, there are basically three types of explosive-forming systems: high explosive, low explosive and explosive gas. Generally, high-explosive forming is performed in an open system, whereas the other two are in closed systems; however, under certain conditions, the high-explosive system can be designed for a closed system also.

The high-explosive forming operation is characterized by a shock-wave energy source, while the other two are characterized by rapid pressure rises, as shown in Fig. 2. The energy-wave duration in high-explosive forming is on the order of microseconds with resulting velocities from 4,000 to 25,000 fps. The duration of the pressure rise time for the low-explosive and gas-explosive systems is on the order of milliseconds with velocities from 1,000 to 12,000 fps.

Most of the explosive forming currently conducted by industry is of the high-explosive type. It is generally performed in an open-pit type operation using water as a transfer medium. Dies are loaded with a part blank and explosive, lowered

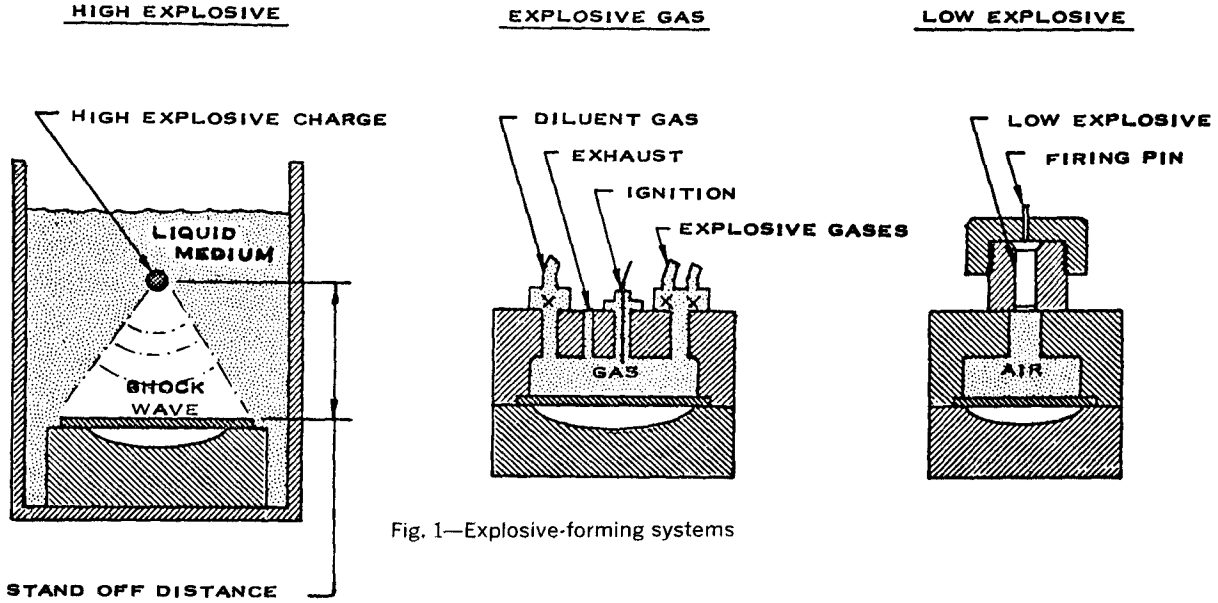

Fig. 1—Explosive-forming systems

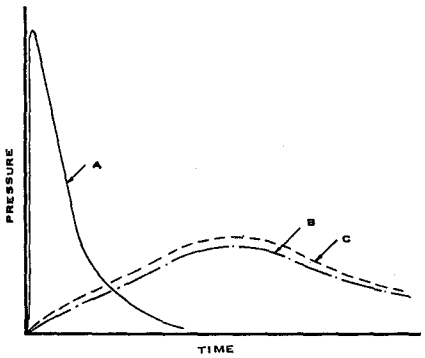

ENERGY WAVE CHARACTERISTICS	A HIGH EXPLOSIVE	B LOW EXPLOSIVE	C EXPLOSIVE GAS
TYPE OF ENERGY WAVE	SHOCK WAVE	RAPID PRESSURE RISE	RAPID PRESSURE RISE
DURATION OF ENERGY WAVE (SECONDS)	10^{-6}	10^{-3}	10^{-3}
VELOCITY OF ENERGY WAVE (FT/SEC X 10^{-3})	4–25	1–8	1–12

Fig. 2—Energy waves for explosive-forming systems

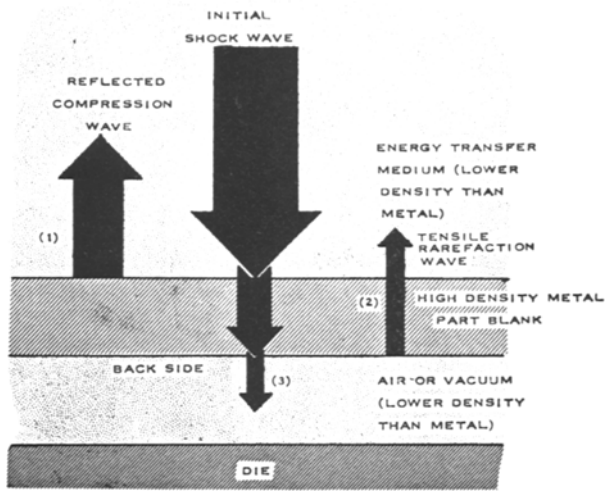

Fig. 3—Transmission and reflection of shock waves

into the water a sufficient depth, and the explosive charge detonated.

The initial shock wave is transmitted through the water to the part as shown in Fig. 3. Because the water is less dense than the metal blank, part of the wave is transmitted through the metal blank and part of it is reflected back through the water as a compressive wave[1] due to the low- to high-impedance match of the water and the blank. This compressive reflected wave is the principal reactive force of the initial shock wave and constitutes the major deformation force for forming the metal blank.

The shock wave transmitted through the metal blank is partially reflected from the back side of the part as a tensile rarefaction[2] due to the high- to low-impedance match of the part and the vacuum, resulting in a reinforcement of the first reflection giving additional forming force, but also causing a metal forming defect known as "scabbing." The nonreflected portion of the wave[3] is transmitted through the part and is absorbed by the die.

In determining the effect the shock wave has on forming, it is instructive to study the wave equation solution of Taylor:

$$\frac{\partial^2 h}{\partial x^2} = \frac{1}{C^2}\frac{\partial^2 h}{\partial t^2} \qquad C = \sqrt{\frac{E}{\rho}} \qquad \text{(Ref. 4)}$$

where C is the tension-shock-wave velocity moving at the speed of sound through the part and toward its center. This velocity is shown to be the square root of the modulus to density ratio. The other variables are shown in Fig. 4 with the expected shapes of a metal disk rigidly clamped around the edge. The solution to the wave equation with

Fig. 4—Effects of shock-wave velocities

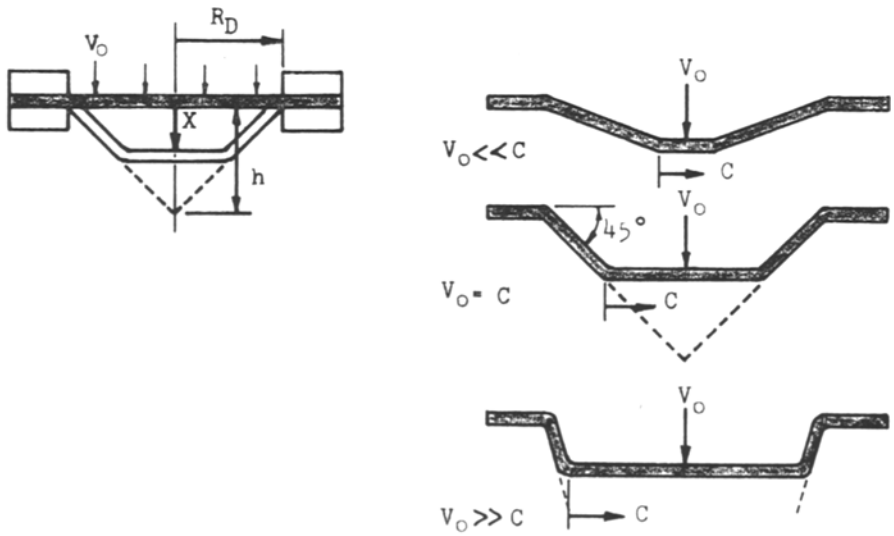

proper boundary conditions is:

$$V_L = {}^1/_2 \frac{h}{R_D} V_0$$

where V_0 is the velocity of the oncoming wave transmitting through the water and V_L is the average velocity at which the cup wall elongates. It can be seen that, as V_0 increases from size of charge, quality of explosive, etc.; the conical shape of the part will change with an increase in the depth-to-diameter ratio (h/R_D). This initial shape from the shock wave has a great influence on formability and the mode of fracture.

Theodore von Kármán[3] developed a theory for the propagation of plastic-strain waves in a bar as an explanation of limiting speed at which deformation can be made in a metal. Starting with the equation of motion in a bar of infinite length which is suddenly put in motion with a constant impact velocity:

$$\rho \frac{\partial^2 u}{\partial t^2} = \frac{d\sigma}{d\epsilon} \frac{\partial \epsilon}{\partial x}$$

where u is the displacement of an element in the x direction, σ is the apparent stress, and ϵ is the strain ($\epsilon = \partial u/\partial x$), the general solution to this equation is:

$$V_c = \int_0^{\epsilon_m} \left[\frac{d\sigma/d\epsilon}{\rho} \right]^{1/2} d\epsilon$$

where ϵ_m is the strain at maximum load. This equation gives a critical impact velocity V_c which is based on an integration of the slopes across an engineering stress–strain curve with respect to the strain. When the impact velocity exceeds the velocity at which plastic strains can propagate, the bar will break near the impacted end with no plastic strain elsewhere in the bar.

Both of the above theories on shape and limitation of deformation have been shown to be fairly accurate in recent Air Force contracts conducted at Ling-Temco-Vought, Inc. These results are shown in some of the following figures. Tensile, tubular and disk-shaped specimens were tested at varying velocities.

Plotting the uniform elongation vs. impact velocity produced a typical curve with five distinct behavior patterns *A*, *B*, *C*, *D* and *E*, as shown in the top schematic of Fig. 5. Under static conditions with a standard tensile-test machine, the ductility is shown at *A* with fracture occurring anywhere along the specimen, generally toward the center. Specimens pulled at slightly higher velocities produced somewhat increased ductility, as shown at *B*, and generally with fracture occurring near the fixed end. Impacting specimens at medium velocities gave a flattening of the ductility curve, as denoted by region *C*, with double necking and fracture at either end. The uniform elongation drops rapidly with velocity beyond a certain "critical velocity," as shown by region *D*. Double necking generally

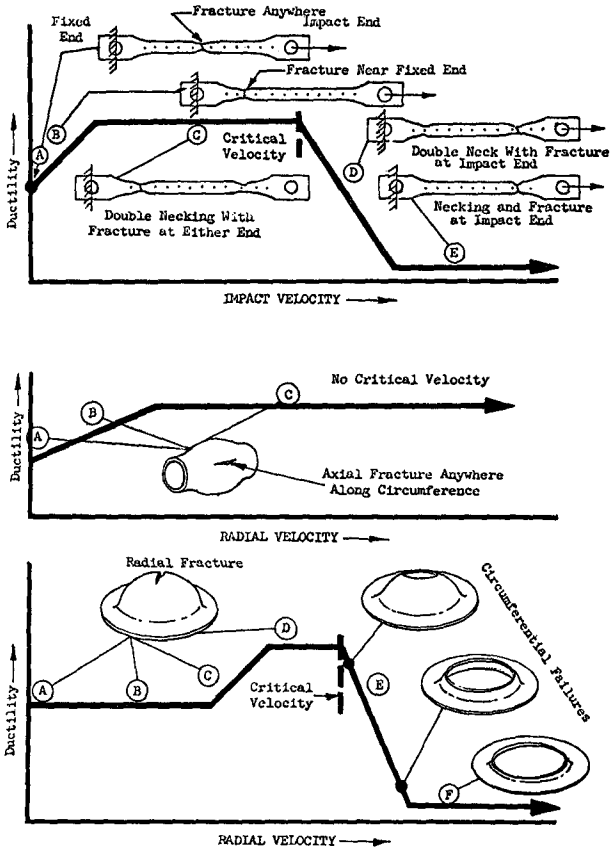

Fig. 5—Ductility curves showing fracture types

continues to occur in this area of testing, but with fracture predominantly taking place near the impacted end. Further increases in test velocity produce negligible ductility across the specimen with fracture consistently at the impact end.[1] In some cases, fracture occurred outside the reduced section of the specimen.

Several significant features can be discussed about the behavior of these specimens impacted at varying velocities. In the first place, ductility can be increased significantly with velocity for most metals and alloys. This results principally from the fact that the shape of the true stress–strain curve changes with velocity. In general, the curve moves upward with increasing velocity, thereby increasing the rate of strain hardening. This produces a stabilizing influence against necking, thereby forestalling the unstable neck and fracture. The second significant feature of this type of a curve is the occurrence of a "critical velocity" beyond which negligible ductility exists. This behavior has been discussed in the literature in some detail,[6, 10, 11] and is based on the propagation of elastic- and plastic-strain waves throughout the length of the specimen. Near the critical, the propagating strain waves build up at both ends of the specimen and result in instability and fracture. Greater impact velocities produce fracture only at the impacted end because the wave velocities are insufficient to propagate the length of the specimen.

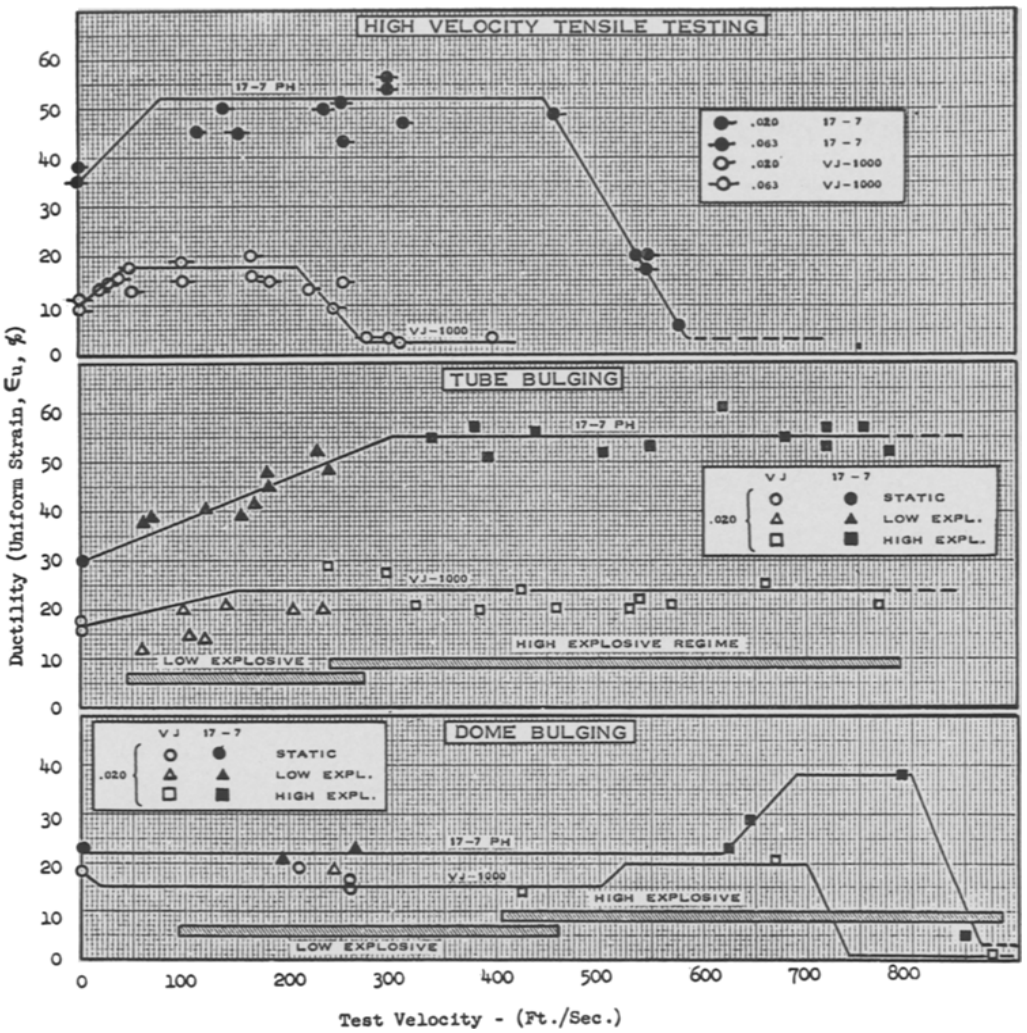

Fig. 6—Typical curves for experimental testing at high speeds

A third significance of the curve is that ductile materials behave in a ductile fashion for all test velocities. Considerable ductility is observed in the necked region, even beyond the critical velocity.[1] This was first observed by Clark and Wood in their early testing.[13]

The middle curve in Fig. 5 illustrates the ductility and fracture phenomena occurring during tube bulging at high speeds. Two-inch-diameter tubing with a 0.020-in. wall thickness was used for testing each material. Region *B* illustrates the highly significant increase in ductility with forming velocity which is very similar to the same occurrence in the tensile specimen. This is generally in the low-explosive forming range. The ductility curve flattens at higher velocities in the high-explosive range. No critical velocity exists for tube bulging, even at extremely high velocities in the upper regions of high-explosive testing. This results from the fact that, due to the nature of the loading, strain waves fail to propagate around the circumference in a manner similar to tensile specimens. Axial fractures occur anywhere around the circumference at all testing velocities.

The lower curve in Fig. 5 illustrates the ductility and fracture phenomena which result from high-speed dome bulging. Six regions, *A*, *B*, *C*, *D*, *E*, and *F*, are shown to exist for this type of forming. The increase in ductility at high velocity is seen to be delayed when compared with the tensile specimen and the tube. The low-explosive region, denoted by *B*, results in the same ductility as under static conditions. Region *C* illustrates a rapid increase in ductility with forming velocity and *D* shows a flattening of the curve. These two regions represent the increased ductility associated with dome bulging at the higher velocities of high-explosive forming. Region *E* illustrates the rapid decline in ductility after a critical velocity has been reached. Radial-type fractures occur below the critical velocity while circumferential fractures occur above the critical. Small disks are blown out of the crown of the dome immediately above the critical. The severed disk increases in size as the velocity is increased above the critical, so that, at a sufficiently high velocity, a disk is sheared that equals the die diameter.

The increased ductility of the dome at the higher velocities results for the same reason as the tensile specimen. The critical velocity is present for the

bulged domes, also for the same reason as for the tensile specimens; however, strains propagating along the original disk diameter reflect from two fixed edges as compared to one for the tensile specimen. This would be similar to pulling a tensile specimen at both ends simultaneously. The dome assumes the shape of a modified truncated cone during forming, with fracture occurring circumferentially around the edge of the truncated flat portion. The principle difference in the dynamics of the tensile specimen simultaneously pulled from both ends and the dome is that the two ends move in the former, while the middle moves in the latter.

Figure 6 illustrates typical experimental data for 17-7 PH stainless steel and Vascojet 1000 tool steel for the tensile test, tube bulging and dome bulging. These curves show the large increase for 17-7 PH and the slight increase for Vascojet 1000 in ductility with increasing velocity. Very little scatter is noted except in the low-explosive tube-bulging range for Vascojet 1000.

A set of composite ductility graphs for a number of materials for tensile testing, tube bulging and dome bulging is shown in Fig. 7. It should be noted that, although the typical graphs in Fig. 5 showed a considerable rise in ductility with forming speed, some of the materials in Fig. 7 indicate no increase in ductility. René 41, 6Al – 4V titanium, 13V – 11Cr – 3Al titanium and molybdenum (0.5% Ti) maintain constant ductility to the critical velocity for tensile testing and dome bulging. A-286 austenitic stainless steel and 6Al – 4V titanium have no increase in ductility with forming velocity for tube bulging. The shape of the stress–strain curve for these materials obviously does not change sufficiently with increased speeds to improve ductility.

The critical velocities are noted to vary considerably for high-speed tensile testing from 125 fps for molybdenum (0.5% Ti) to 435 fps for 17-7 PH stainless steel. The theoretical critical velocity determined by von Kármán's analysis is shown to be in slight variance with the absolute critical velocities. The principle reason for this is that the theoretical critical velocity is based on static stress–strain curves, while the absolute critical is based on dynamic conditions.

The critical velocities for the bulging of domes is shown to be somewhat higher than the tensile specimens. This is because the test velocity for the dome was measured in the direction of dome movement and not in the plane of the sheet metal. The critical velocities for all materials are shown to be in approximately the same order for the domes and tensile specimens.

Highly significant features of formability can be gained by observing the tube and dome-bulging composites of Fig. 7. It is apparent that A-286

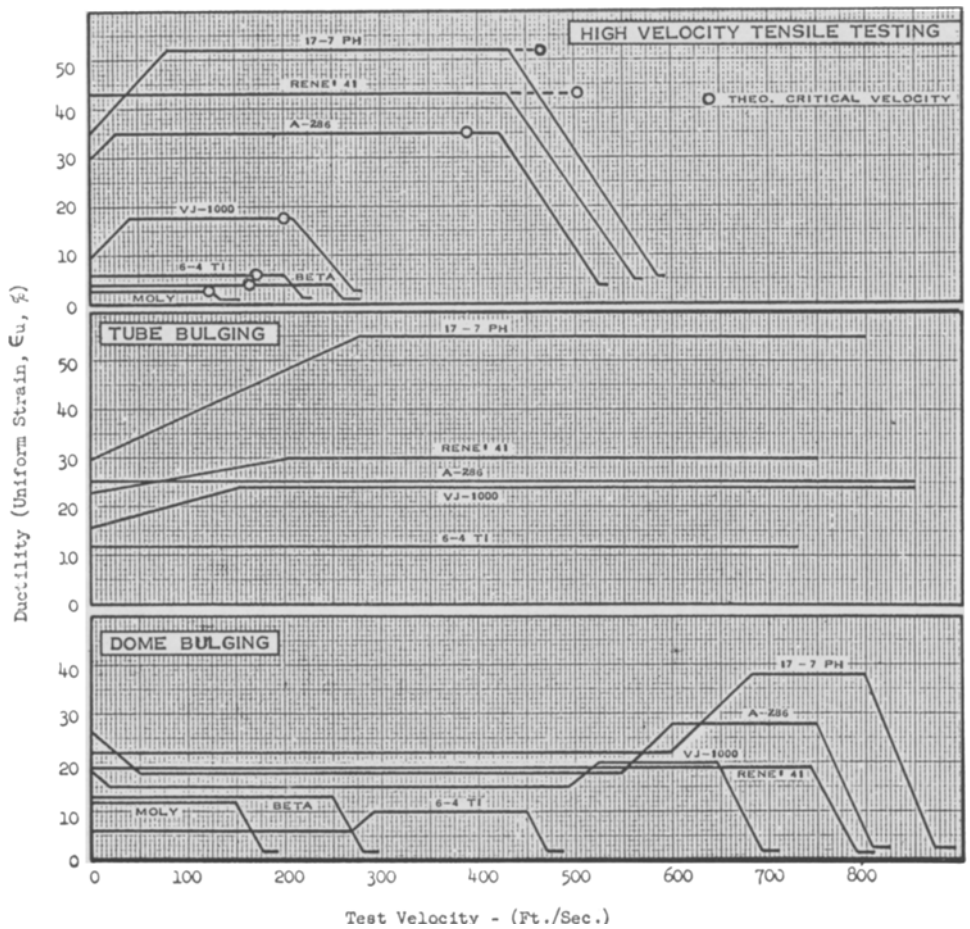

Fig. 7—Variations in ductility with testing velocity

stainless steel and 6Al – 4V titanium can be equally formed by all processes for tube bulging because of the flatness of the curves; however, the upper ranges of low-explosive forming and all high-explosive forming produce superior formability for tube bulging of 17-7 PH stainless steel, René 41 and Vascojet 1000 tool steel. This would mean that these materials are also very formable by the capacitor-discharge forming methods. In dome bulging, it can be observed that 17-7 PH, A-286, Vascojet 1000 and 6Al – 4V titanium have improved formability in the high-explosive ranges of velocity. The low-explosive bulging produces the same formability as under static conventional processes for the other materials. Actually, A-286 and Vascojet 1000 show reduced formability under low-explosive conditions. It is felt that this occurred from lack of protection of the part from the burning propellant, producing localized hot spots.

Most of the discussion so far has been related to forming by stretching. Although this is a very important part of explosive forming, there is also another part resulting from drawing of sheet metal between the die and a pressure ring. This is particularly true for the bulging of a disk into hemispherical domes, flat-bottom domes and other shapes. As the disk is drawn radially toward the center, the outer periphery is placed in hoop compression, resulting in buckling instability for thin-gage parts. These buckles can be transmitted across the drawn flange to the unsupported dome wall in the spherical shaped part as shown in Fig. 8.

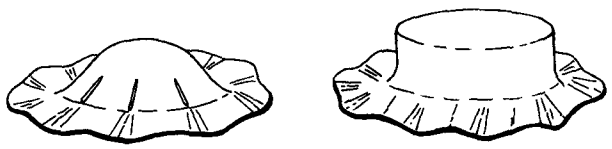

Fig. 8—Buckling in explosive forming

Formability-limit curves have been developed for these type parts on the previously mentioned Air Force contracts.[1, 2] A typical schematic is shown in Fig. 9. It is shown that a considerably greater formability is obtained when the tooling combines the drawing with the stretching operation. Also, it should be noted that for thin-gage parts beyond a critical H/t, total formability is reduced to that obtained with rigid clamping of the flange. This critical H/t value is approximately 100 for most materials; however, it is as low as 50 for materials such as aluminum.

References

1. *Wood, W. W., et al., "Final Report on Sheet Metal Forming Technology," Volumes I and II, Contract AF 33(657)-7314, ASD Project No. 7-871 (July 1963).*
2. *Wood, W. W., et al., "Advanced Theoretical Formability Manufacturing Technology," Contract AF 33(657)-10823, ASD Project No. 8-143 (November 1964).*
3. *von Kármán, T., "On the Propagation of Plastic Deformation in Solids," OSRD Report No. 365 (NDRC Report A-29) (January 28, 1942).*
4. *Taylor, G. I., "Plastic Wave in a Wire Extended by an Impact Load," Scientific Papers,* **1,** *Cambridge University Press (1958).*
5. *Duwez, P. E., "Preliminary Experiments on the Propagation of Plastic Deformation," NDRC Report A-244 (OSRD No. 3207) (February 1944).*
6. *von Kármán, T., Bohnenblust, H. F., and Hyers, D. H., "The Propagation of Plastic Waves in Tension Specimens of Finite Length; Theory and Method of Integration," OSRD Report No. 946 (NDRC Report A-103) (Ocotber 15, 1942).*
7. *Bohnenblust, H. F., Charyk, J. V., and Hyers, D. H., "Graphical Solutions for Problems of Strain Propagation in Tension," OSRD Report No. 1204 (NDRC Report A-131) (January 21, 1943).*
8. *Riparbelli, C., "On the Relation Among Stress, Strain and Strain Rate in Copper Wires Submitted to Longitudinal Impact," Proc. SESA,* **14,** *55 (1954).*
9. *Sternglass, E. J., and Stuart, D. A., "An Experimental Study of the Propagation of Transient Longitudinal Deformations in Elasto-plastic Media," J.A.M.,* **20,** *Trans. ASME,* **75,** *427 (1953).*
10. *Malvern, L. E., "The Propagation of Longitudinal Waves of Plastic Deformation in a Bar of Material Exhibiting Strain-rate Effect," J.A.M.,* **18,** *Trans. ASME,* **73,** *203–208 (1951).*
11. *Hauser, F. E., Simmons, J. A., and Dorn, J. E., "Strain Rate Effects in Plastic Wave Propagation,"* **133,** *3, Metals Research Laboratory, University of California (June 1960).*
12. *Pearson, J., "Application of Critical Impact Velocity Data to the Explosive Forming of Sheet Metal Parts," High Energy Rate Metal Forming, Interim Report No. 5, Appendix I, 209.*
13. *Clark, D. S., and Wood, D. S., "The Tensile Impact Properties of Some Metals and Alloys," Trans. ASM,* **42,** *45 (1950).*
14. *White, M. P., and Griffis, L., "The Permanent Strain in a Uniform Bar Due to Longitudinal Impact," OSRD Report No. 742 (NDRC Report A-71) (July 1942).*

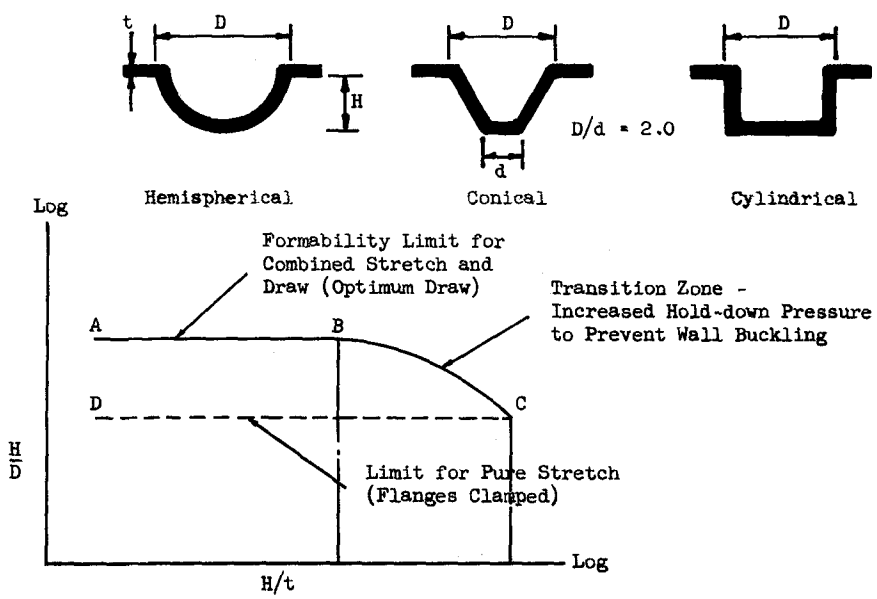

Fig. 9—Forming-limit curve in deep recessing